
**CALCITE NANOPARTICLES AS POSSIBLE
NANO-FILLERS FOR REINFORCING THE
PLASTER OF PALAZZETTO ALESSANDRO LANCIA
IN ROME**

**Federica Valentini^{1,*}, Federica Bertini¹, Marilena Carbone¹,
Riccarda Antiochia², Gabriele Favero³, Aldrei Boaretto¹ and
Delia Gazzoli²**

¹ *Dipartimento di Scienze e Tecnologie Chimiche, Università Tor Vergata, via della Ricerca Scientifica 1, 00133 Roma, Italy*

² *Dipartimento di Chimica, Sapienza Università di Roma, Piazzale Aldo Moro 5, 00185 Roma, Italy*

³ *Dipartimento di Chimica e Tecnologie del Farmaco, Sapienza Università di Roma, Piazzale Aldo Moro 5, Roma, Italy*

(Received 21 March 2015, revised 10 July 2015)

Abstract

In this paper, CaCO₃ nanoparticles were synthesized and then applied on the plaster of Palazzetto Alessandro Lancia, in Rome. CaCO₃ (A) and CaCO₃ (B) were fabricated by using urease enzyme and the miniemulsion strategy, respectively. Samples A and B were characterized by Transmission Electron Microscopy, X-Ray Diffraction and Scanning Electron Microscopy. Then, the dispersions were applied on the plaster and the SEM equipped by the Energy Dispersive X-Ray Analysis was used for characterization. Interesting results were obtained in recovering the mechanical properties of the plaster, not altering their permeability to water and perfectly keeping the wall transpiration but only in presence of nanostructured Calcite (A). This latter resulted in a high quality sample, if compared with the CaCO₃ (B) (that also contains Vaterite compound).

Keywords: nanotechnologies, plaster, restoration, preservation, porous materials

1. Introduction

Nanoscience has opened up enormous potential for cultural heritage conservation, thanks to the unique properties that the reduction in particle size conferred to nanomaterials compared to their micrometric counterparts. Nanostructures are formed by clusters of a few thousands of atoms and show particular properties due to the high area/volume ratio of the clusters, such as high hardness, super-plasticity effects, increase in diffusivity and in dielectric

*Corresponding author, e-mail: federicavalentini.chem@gmail.com

properties [1, 2]. Applications of nanotechnology to wall painting, stones and other art work surfaces conservation have recently provided clear evidence of the huge potentiality of this new science for conservation and preservation of cultural heritage [3, 4]. Nevertheless, the restoration of cultural heritage is still based on traditional methodologies and conventional products which show a lack of compatibility with the original substrates, poor durable performance upon changes of environmental conditions and toxicity effects for the 'end-users' as restorers and conservators [5]. Stones, plasters, wall paintings and many other substrata are susceptible to degradation caused by salt crystallization, often as a result of water evaporation at the interface. This process causes a volume expansion which can cause lifting and detachment of the paint layer or cracks of the plaster [6], compromising thus its conservation.

During restoration treatments, most interventions allow the reinforcement of the porous structure and the consolidation of the surface layer of the artwork. After consolidation, eventual protective treatments confer longer lifetime for the artworks reducing the degradation from pollutants and water condensation. Obviously, all the applied chemicals should ensure maximum durability and chemical inertness and should be compatible with the original substrate. Aside from organic materials from natural origin such as shellac or natural gums available since ancient times and still employed as consolidating agents during restoration practice, over the last decades, polymers, mainly acrylic resins, alkali silicates and silicon esters have been widely used to consolidate stones, plaster, wall paintings and to confer protection and hydro-repellence to the substrata. However, contrary to the expectations, polymers used for the protection of these surfaces have induced further degradation of the artworks and their chemical modifications, such as cross-linking, not only disrupts the readability of the painting but also strongly hamper their removal [7-9]. For these reasons the use of inorganic materials, compatible with substrata, minimizes the risks and prevents unexpected side effects. In addition, inorganic consolidating and filler agents preserve the wall porosity and therefore ensure long-lasting wall painting consolidation, permeability to moisture evaporation as in the wall before treatment and most of them do not hinder subsequent restoration. Ferroni and Dini [10, 11] elaborated a method to clean and consolidate stones, wall paintings and plasters affected by sulphatization and/or crystallization of other salts based on a *carbonation* reaction. In their approach the original binder ($\text{Ca}(\text{OH})_2$) is *in situ* produced and begins a very slow setting process, just called *carbonation* (where the calcium hydroxide reacts with the carbon dioxide of the air producing calcium carbonate), that slowly increases the cohesion of the paintings. $\text{Ca}(\text{OH})_2$ nanoparticles treatment is the logical evolution of the Ferroni-Dini method, and can replace it in most cases with some advantages. For examples, the nanometric size of the particles assures a good penetration into the porous matrix of the stones or plasters (to be consolidated), and the lowering of the possible whitening effects. Recently, many works are published concerning the applications of $\text{Ca}(\text{OH})_2$ nanoparticles for the restoration of frescoes [12], wall paintings [13] and also for the deacidification of paper and canvas [14]. Instead,

the approach based on the use of nano-CaCO₃ as filler for the restoration and conservation of plaster appears to be much less studied [15]. For this purpose, the research aim of this work is the study of the analytical performances of the CaCO₃ as nano-filler for the damaged plasters, collected on Palazzo Alessandro Lancia, in San Salvatore in Campo, Rome (Italy). The facade of the Palazzo Lancia needs to be restored and preserved because it represents one of the most important Renaissance Roman buildings (that are about 200 throughout Rome) showing the typical plaster with fresco painting or graffiti decorations [16, 17]. The reason to apply CaCO₃ as nano-filler is justified on the basis of kinetic considerations because the spontaneous carbonation is a very slow mechanism for consolidation of plaster and/or natural limestone. For this purpose CaCO₃ nanoparticles are synthesized, characterized (applying several analytical techniques, as: FE-SEM/EDAX; HR-TEM/EDAX; XRD; FT-IR; μ -Raman) and finally applied on the plaster of Palazzo Alessandro Lancia. The resulting analytical performances (on the plaster samples, before and after the treatments) are compared with that exhibited by several other nano-fillers and consolidating agents, widely described in literature [18].

2. Experimental

2.1. Materials and reagents

All the reagents, including calcium carbonate, sodium carbonate, calcium chloride, calcium chloride anhydrous, magnesium chloride and urea phosphate were of analytical grade (Sigma-Aldrich, Buchs, Switzerland). The enzyme urease, type III, from Jack Beans was purchased from (Sigma-Aldrich) and sodium dodecyl sulphate, SDS, from Merck (Germany). All other chemical reagents were of analytical grade and used as received. CaCO₃ nanoparticles were synthesized by using two different methods: A. (enzymatic approach) and B. (mini-emulsions technique), widely described in literature [19, 20], respectively.

2.2. Filler based treatment using the CaCO₃ nanoparticles

In order to evaluate the treatment efficiency, 1 mg/mL CaCO₃ alcoholic suspension (in 2-propanol, as working medium) was applied on six plaster samples (5x5x2.5 cm³). Before to start with the restoration treatments, 1 mg/mL alcoholic suspension was subjected to the ultrasonication procedure, for 3 hours. The treatment was carried out, in laboratory conditions (T = 25°C and R.H. 45%), applying the alcoholic dispersion by brush only on half of the surfaces, leaving untreated the other one for comparison. The CaCO₃ alcoholic dispersion was applied brushing 1 mL of the suspension on the dried plaster surface; the procedure was consecutively repeated 10 times, during one month, after solvent evaporation. In this way, about \approx 10 mg of CaCO₃ were loaded on each plaster sample surfaces during the first month, and about 60 mg of CaCO₃ for the entire

duration of the experiment, equal to 6 months (i.e. 180 days, where a stable reinforcing and filling of the micro-fractures was achieved, demonstrated later in the text, by the STT (Scotch Tape Test) measurements [ASTM D3359-02: *Standard Test Methods for Measuring Adhesion by Tape Test*, ASTM International, 10 August, 2002].

2.3. Apparatus and procedure

TEM analysis were performed using a JEM-2100 (JEOL, Japan) operating at 200 kV accelerating voltage, equipped with an energy dispersive X-ray spectrometer (EDAX, Oxford, UK) suitable for element identification. A small drop of the dispersion was deposited on a 200 mesh carbon coated copper grid, which was putted into the TEM chamber analysis after complete solvent evaporation.

FE-SEM/EDAX investigation was performed by using a FE-SEM/EDX-LEO 1550 equipped with energy dispersive X-ray analyser. Samples were supported on stubs by carbon paints and were coated by gold. The accelerating voltage ranged between 20 and 30 kV during SEM measurements, while it was set at 25 kV for EDAX analysis. XRD (X-Ray Diffraction) measurements were carried out by using Philips X'Pert Pro MRD with Cu K α radiation ($\lambda = 1.542$ nm) under a voltage of 40 KV and a current of 40 mA in the 2θ angular range between 20° and 80° . SAXS (Small Angle X-Ray Spectroscopy) was carried out by using a Bruker AXS Nanostar-U instrument, equipped by the Cu K α radiation emitted by a rotating anode source, working at 40 kV and 20 mA. Nanoparticle dispersions are inserted in 2 mm capillary tubes and analyzed for 5000 s. Measurements were performed at R.T. on a two dimensional detector, placed at the distance of 1.06 m. FT-IR analysis was performed by an FT-IR Thermo-Nicolet Nexus spectrophotometer with an acquisition time of 100 seconds and resolution of 5 cm^{-1} . Raman spectroscopic analyses were carried out in the back-scattering geometry with an in Via Renishaw Micro-Raman spectrometer, equipped with an air-cooled CCD detector and edge filters. A 488.3 nm emission line from an Ar $^+$ ion laser was focused on the sample under a Leica DLML microscope, using a 20 \times objective. Ten 10s or 20s accumulations were generally attained for each sample with an incident beam power of about 5 mW. The resolution was 2 cm^{-1} and spectra were calibrated using the 520.5 cm^{-1} line of a silicon wafer. Data analysis included baseline removal and curve fitting, using a Gauss-Lorentz cross-product function by Peakfit 4.12 software (Jandel, AISN Software).

The porosity of the plaster was measured by a mercury intrusion porosimeter, Carlo Erba Porosimeter4000. Water Capillary Absorption (WCA) of plaster samples was measured by gravimetric sorption technique [Commissione 'Beni Culturali-NORMAL', *Materiali lapidei naturali ed artificiali, Determinazione dell'assorbimento d'acqua per capillarità*, UNI 10859, 2000.], while colour variation was determined using a SP 820 λ /830 λ spectrophotometer. In this system, the colour is represented as a position in a

three-dimensional sphere where the vertical axis L represents the lightness (ranging from black to white), and the horizontal axes indexed as a and b, are the chromatic coordinates (ranging from a: greenness to redness and b: blueness to yellowness). The total colour difference (ΔE) is calculated using the equation, reported below:

$$\Delta E = \sqrt{\Delta L^2 + \Delta a^2 + \Delta b^2} \quad (1)$$

According to the Hunter system [EN 15886:2010, Conservation of cultural property – Test methods – Colour measurement of surfaces] L, a, and b values were averaged from ten readings across each plaster sample, on different position of samples [21]. For comparative studies we used an original plaster without damages from the ISCR (Istituto Superiore Centrale per il Restauro) in Rome, half of the plaster sample that was not subjected to any nano-filler treatments. Total colour differences were calculated for treated plaster samples.

3. Results and discussion

3.1. The case study of the Palazzetto Alessandro Lancia in Rome

The status of conservation of Palazzetto Alessandro Lancia, located in Largo Argentina in Rome (latitude is 41.89477 and longitude is 12.49328) is illustrated for two different areas homogeneously distributed on the entire surface of the façade. One area (Figure 1a) was restored during the 1950; the second one probably before 1950 [22, 23]. During the restoration and consolidation past events several kinds of consolidants have been applied on the plaster surface as ammonium oxalates [24] and others [25]. These areas, mainly located in the lower zone of the facade and specifically below the first and second string-course, evidence the presence of several parts subjected to the puttying. Regarding the state of preservation, a second mapping of the facade of the plaster and plaster finish has been also reported on Figure 1b. There it is evidence that this surface was heavily etched, affected by delamination and by several detachments of the plaster finish. The detachments are characterized by bubble lifting especially located in the central area of the facade, in the vicinity of the emblem. From these damaged areas, where several detachments are present, probably because the ammonium oxalate treatment did not work, the new restoration treatment based on CaCO_3 nano-filler (dispersed in alcoholic medium) has been applied. For this purpose, ten detached plaster fragments (Figure 1c, fragments not more replaceable) were used for this study. An original reference sample (from ISCR, Rome) without damages was used for comparison.

3.2. Physicochemical characterization of nanoparticles

The XRD pattern recorded for the CaCO_3 (A) nanoparticles obtained by the urease-based-synthesis approach matches that of CaCO_3 in the calcite modification, according to the JCPDS-International Centre for Diffraction Data

[26], Figure 2 (black profile). The XRD profile obtained on the CaCO_3 (B) sample, Figure 2 (red profile), shows the presence of CaCO_3 in the calcite and the Vaterite modifications [26] and of magnesium chloride (< 0.3% w/w). The latter compound represents the residual amount of the precursor used for the synthesis of CaCO_3 nanoparticles performed by the mini-emulsions technique.

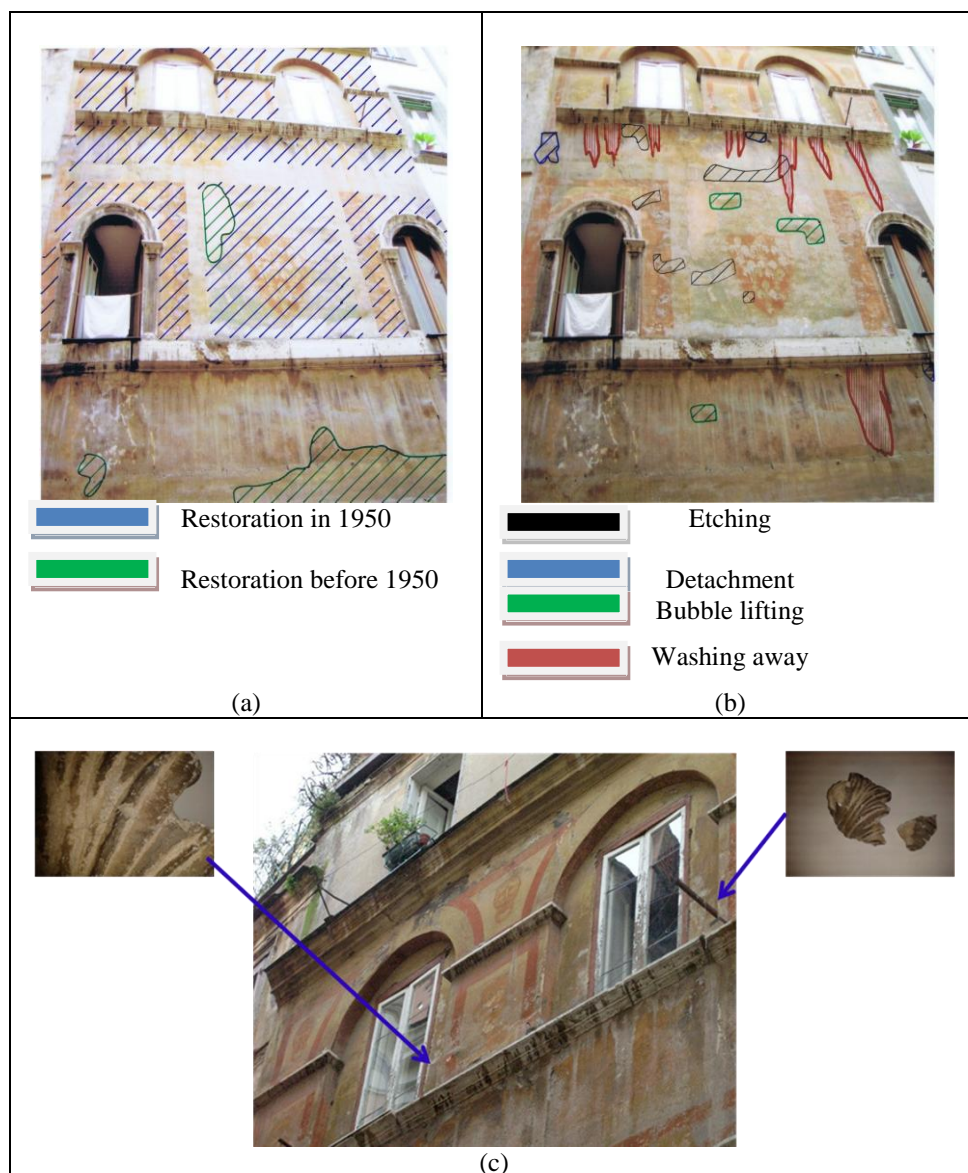


Figure 1. Photographs and mapping of Palazzo Alessandro Lancia, in Rome: (a) different areas restored 1950 (marked in blue), or before 1950 (marked in green) and other original ones; (b) status of conservation in the case of the plaster and the plaster finish; (c) no more replaceable detached plaster fragments used for our investigation.

According to these results, only the CaCO_3 (A) is selected for the plaster based filler treatments. The results were also confirmed by the FT-IR investigation (data not shown).

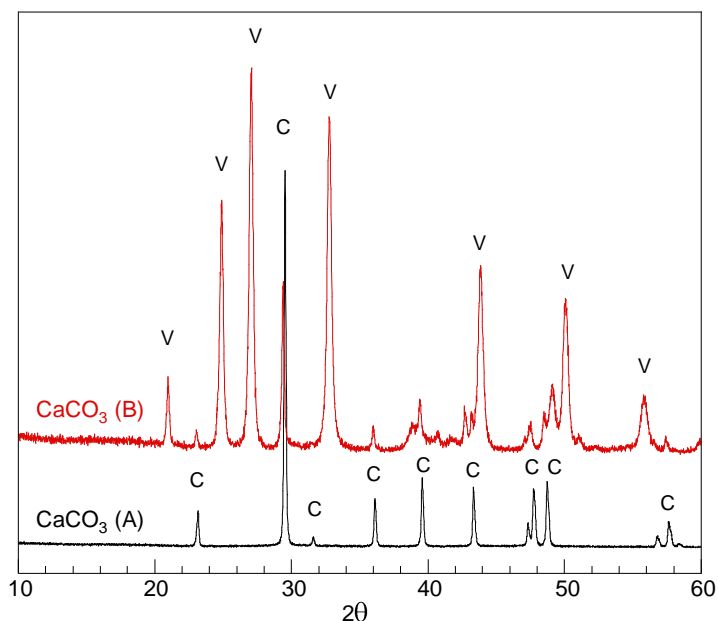


Figure 2. XRD spectra for CaCO_3 (A) and CaCO_3 (B) samples. Spectra shifted for clarity. Peaks coded as C and V are characteristic of Calcite and Vaterite, respectively.

TEM study was carried out using completely dried samples for CaCO_3 nanoparticles, obtained from the alcoholic dispersion and then deposited by the solvent casting technique, on the TEM grid and leaving the solvent to evaporate. It is well known that the drying process onto the TEM grid support looks a lot like the drying natural processes within the interstices of the external plaster surfaces. TEM characterization was applied to have information about particle size, shape and crystalline structure and to study the agglomeration status of the nanoparticles as a function of the sample preparation for TEM investigation. The HR-TEM micrographs of CaCO_3 (A) nanoparticles show spherical particles having diameters ranging from 10 to 16 nm (Figure 3b).

The majority of the nanoparticles have diameter below 100 nm (Figure 3a), in agreement with the SAXS (Small Angle X-Ray Scattering) measurements (data not shown). However there are few aggregates having a size greater than 100 nm and this can depend on the agglomeration that occurs upon solvent evaporation. In the corresponding EDAX spectrum (Figure 3c) calcium is the most abundant element in the sample, with the presence of phosphorus (which comes from urea phosphate, the enzymatic substrate) and magnesium (from MgCl_2 inorganic precursor). The trace elements of Cu as well as of C (high amount) come from the Cu grid ($\phi = 3\text{mm}$) coated with carbon tape used for the measurements, whereas Oxygen/O comes from the laboratory atmosphere.

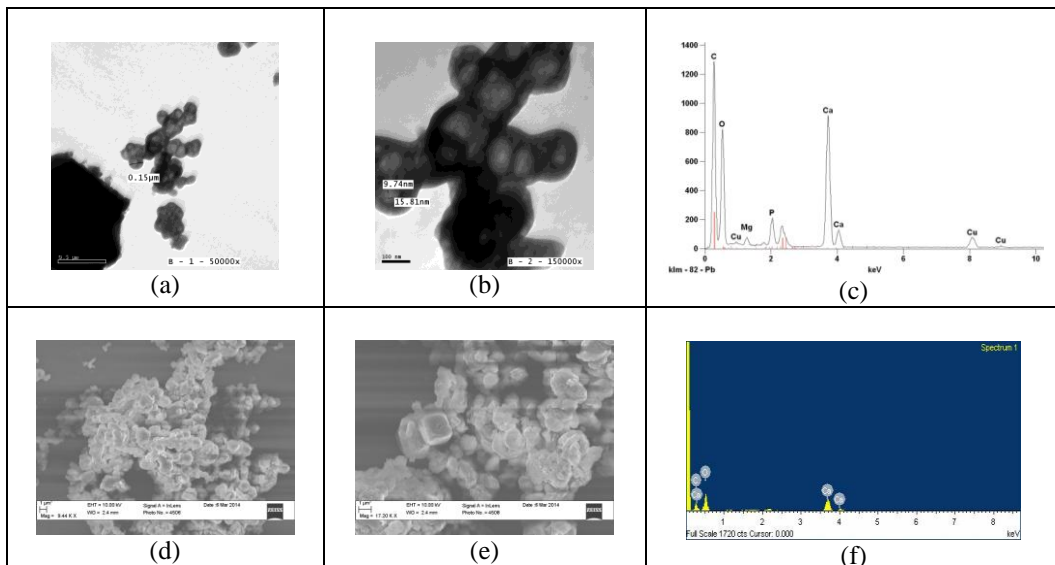


Figure 3. (a) HR-TEM micrograph of CaCO_3 (A) at magnification of 50000X; (b) HR-TEM micrograph of CaCO_3 (A) at magnification of 150000X; (c) EDAX spectrum of the CaCO_3 (A) sample; (d) FE-SEM micrograph of CaCO_3 (A) at magnification of 17.20KX; (e) FE-SEM micrograph of CaCO_3 (A) at magnification of 9.44KX; (f) FE-SEM/EDAX microanalysis for the sample (A).

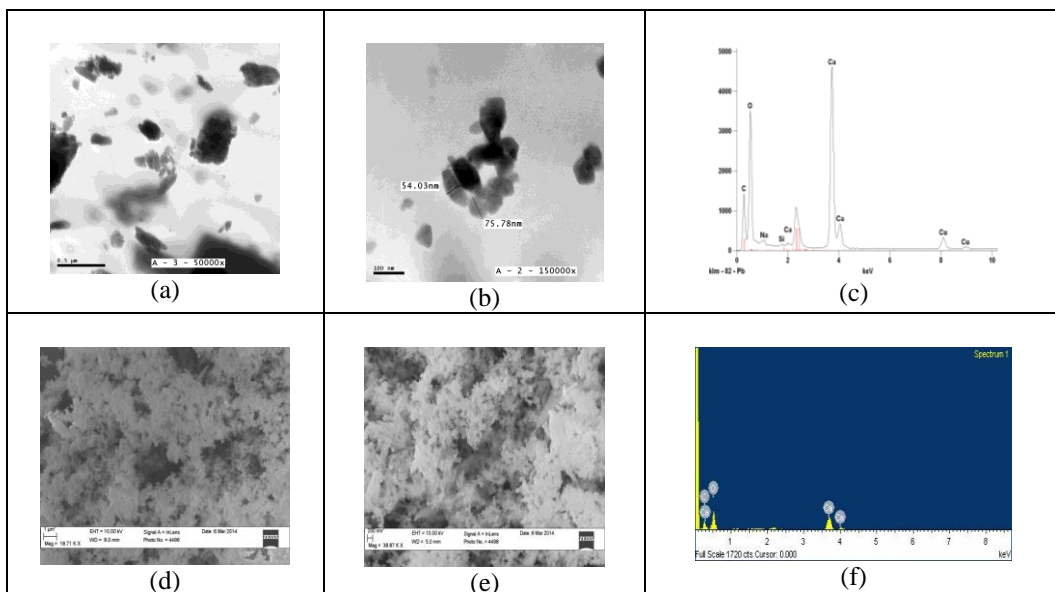


Figure 4. (a) HR-TEM micrographs of CaCO_3 (B) at magnification of 50000X; (b) HR-TEM micrographs of CaCO_3 (B) at magnification of 150000X; (c) the corresponding EDAX spectrum; (d) FE-SEM micrograph of sample (B) at magnification of at magnification of 18.71 KX; (e) FE-SEM micrograph of sample (B) at magnification of at magnification of 18.71 KX; (f) EADX microanalysis spectrum of sample (B).

SEM images of the dried samples reveal larger aggregates of pure calcite CaCO_3 (Figure 3d and 3e acquired at different magnification), characteristic of screw growth rombohedral incorporated in twin structures, according to literature findings [19] and also to the SAED data (SAED not shown here).

EDAX analysis (Figure 3f) confirms the elemental composition of pure calcite also highlighted on Figure 3c. The lack of certain elements detection can be due to the SEM preparation of the sample—and/or to the FE-SEM/EDAX instrument sensitivity.

For the CaCO_3 (B) sample (method B, mini-emulsions strategy) the HR-TEM micrographs show the presence of several platelet-like nanoparticles (Figure 4a). There are several aggregated platelet-like nanoparticles with diameters less than 100nm (Figure 4b), according to the SAXS results (data not shown here). In the same sample, agglomeration with size larger than 100nm have been also highlighted. In the corresponding EDAX spectra (Figure 4c) Ca is the main element present in the sample, but also C, O and Cu are present, similarly to that observed in the case of CaCO_3 sample (A). The difference in the EDAX spectrum of CaCO_3 (B) is the additional presence of Na element, probably related to the SDS precursor, used for the mini-emulsion based synthesis approach. SEM micrographs of the dried and washed samples reveal larger aggregates of platelet-like nanoparticles (Figure 4d and 4e acquired at different magnification), as expected when the solvent evaporates from the samples. The FE-SEM/EDAX microanalysis of sample (B), Figure 4f, shows the same elements than that recorded for sample (A). Na element is not recorded probably because the SEM/EDAX is less sensitive than the HR-TEM/EDAX (Figure 4c).

3.3. Characterization of the plaster samples after CaCO_3 nanoparticles treatment

According to the above described results, only the CaCO_3 (A) is pure calcite and for this purpose the sample (A) was applied, as filler, on the plaster fragment surfaces.

In order to assess that CaCO_3 acts as filler for the damaged plaster samples, the Hg based porosimetry analysis has been carried out. The original plaster/intonaco (from the ISCR source) presents pores with a diameter ranging from 0.0037 μm to 150 μm . After accelerated ageing, all samples show an increase in total open porosity (i.e.; 0.053-500 μm) due to the thermal cycling [27]. So the small CaCO_3 (A) particles (having diameters ranging from 9 nm to 150 nm) seem to be an eligible candidate to fill the pores of the damaged plaster samples. In fact, after the CaCO_3 treatment, the plaster porosity results quite similar to that of the original intonaco (0.0062-204 μm vs. 0.0037-150 μm of the standard plaster, from ISCR) meaning that our nanoparticles are able to fill the larger pores, created after the accelerating ageing. The water capillary test was also performed in order to understand the plaster substrata behaviour towards water. The water amount absorbed by plaster surfaces, before and after the

treatment, in terms of the percentage variation (ΔQ) shows interesting results. For the treated plaster fragments, ΔQ reaches a value of -20%, if compared with a ΔQ value of -4% in the case of untreated plaster fragments. The plaster fragments, characterized by pores wider than 1000 Å, could successfully be filled by the CaCO_3 nanoparticles that are suitable to minimize the water adsorption phenomena (0.14 g/cm^2 evaluated before and after the filler based treatment). This behaviour is similar to other case of studies, reported in literature [28], where the pore wall's porosity and their water exchange capacity remain unaltered, indicating that no occlusion effects occurred in presence of the treated plaster fragments. This means that a good transpiration mechanism was preserved, as required for good consolidants and/or filling agents [29].

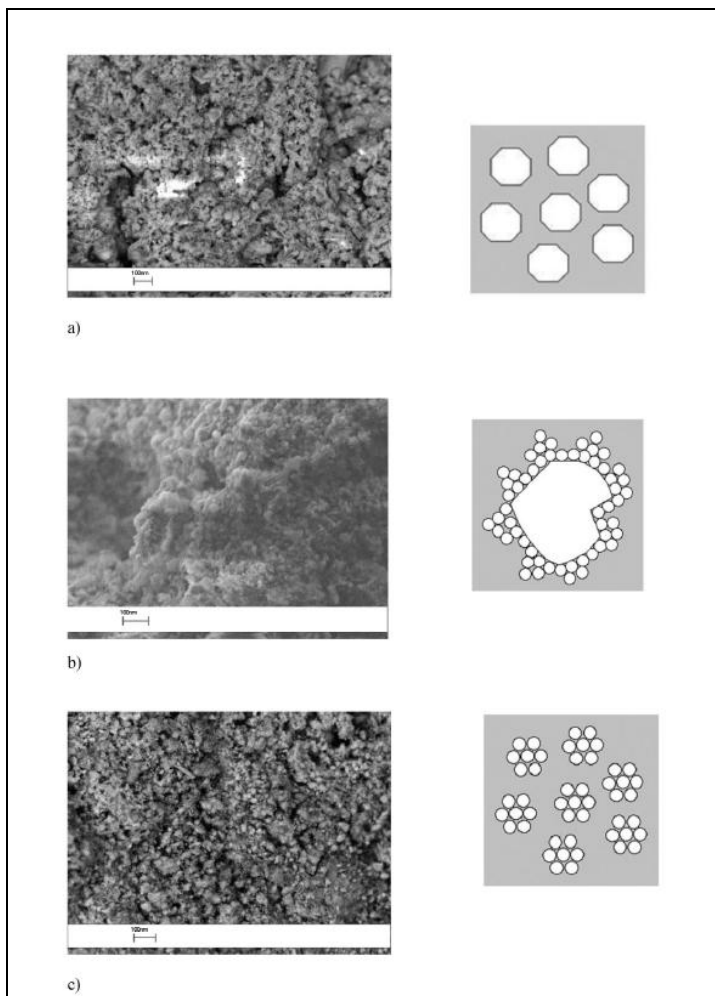


Figure 5. Sequence of plaster fragments: (a) untreated plaster; (b) plaster sample treated by the CaCO_3 nano-filler after 1 month (10 mg, applied by brush); (c) plaster sample treated by the CaCO_3 after 6 months (around 60 mg, applied by brush).

To evaluate the superficial filler effect of the treated plaster samples, the conventional ‘Scotch Tape Test’ (STT) [30] was also carried out. The results obtained showed how ‘weak’ was the surface when an adhesion force was acting on it (using the glue or the scotch tape approaches [31]). Observing the fragments after the STT test it can be possible to verify that the restoration works very well, especially because of the amount of CaCO_3 removed from the plaster fragment surfaces is negligible. In order to evaluate the performances of the CaCO_3 based treatment, under a quantitative point of view, the amount of material taken away (expressed in mg/cm^2 ; where the value is normalized to the surface of the scotch tape) was represented in a graph as a function of number of applications on the selected area of the plaster fragments (this latter containing evident micro-fractures). The graph quantitatively confirms the visual inspection (data not shown). The materials removed from the surface before and after the treatments (indicated as $\Delta\text{M}\%$), demonstrates that the nano-filler treatments result more efficient ($\Delta\text{M} \geq -80\%$) for the plaster fragments. Similar results have been reported in literature by other authors [32].

The CaCO_3 based treatments are effective for the damaged plaster samples probably because of the 2-propanol working medium is able to disperse the CaCO_3 nanoparticles and allow a better penetration through the plaster pore network. Changes of the surfaces due to the CaCO_3 filler treatments, monitored by Scanning Electron Microscope (SEM) at defined time intervals, indicate that an homogeneous coverage is achieved especially after 180 days of exposure to CaCO_3 nano-filler (Figure 5). This is also confirmed by the Ca/Mg ratio values extrapolated from EDAX spectra, acquired before and after the CaCO_3 based treatments. On each fragment samples, 10 measurements were performed on $200 \mu\text{m} \times 200 \mu\text{m}$ areas. The highest values of the Ca/Mg ratio ($\text{Ca}/\text{Mg} = 2.88 \pm 0.03$) after the CaCO_3 based treatment (if compared with the untreated plasters fragments: $\text{Ca}/\text{Mg} = 1.25 \pm 0.01$) demonstrate that an higher Ca content is present on the surface layer of the plaster fragments, meaning that the filling activity of the CaCO_3 nanoparticles was successful.

The presence of CaCO_3 nanoparticles in the plaster structure was also detected by Raman spectroscopy. The ability of Raman spectroscopy to identify crystalline structures and its sensitivity to size, orientation and shape of the structures [33, 34] is further improved when including in the spectral analysis the lattice phonon region (typically $< 400 \text{ cm}^{-1}$). Lattice phonon modes, involving translations and rotations of units within the crystal, show a strong dependence of the crystal organization.

The Raman spectrum collected on the original fragment (Figure 6, curve a) fully matches the one expected for CaCO_3 in the calcite modification [35, 36]. According to group theory, carbonate ions internal modes are expected at about 1085 cm^{-1} (A_{1g} ; ν_1 , symmetric stretching), 715 cm^{-1} (E_g ; ν_4 , in-plane bending) and 1440 cm^{-1} (ν_3 , anti-symmetric stretching). Lattice vibration modes, involving the libration and the translation motion of the carbonate ions, are predicted at about 155 and 280 cm^{-1} , respectively.

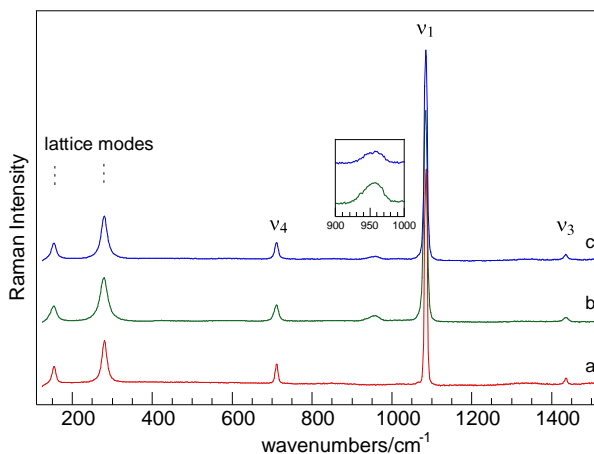


Figure 6. Raman spectra collected on: (a) plaster fragment from Palazzo Lancia; (b) CaCO_3 (A) nanoparticles and (c), plaster fragment after the filling treatment with the CaCO_3 (A) nanoparticles. The inset plot, shows a zoom of the region centered around 955 cm^{-1} attributed to the $\nu_1(\text{A}_1)$ mode of phosphate groups, belonging to urea phosphate enzymatic substrate.

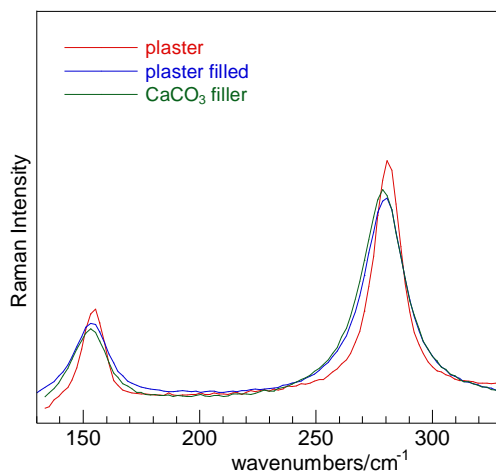


Figure 7. Lattice phonons regions of all the materials. Normalized intensities to the intensity of $\sim 1085\text{ cm}^{-1}$ band.

The Raman spectra of synthesized $\text{CaCO}_3(\text{A})$ (Figure 6, curve b) and of the fragment after filling treatment with the CaCO_3 (A) nanoparticles (Figure 6, curve c) compared well with that of the original fragment. In these spectra a low intensity band centered at about 955 cm^{-1} attributed to the $\nu_1(\text{A}_1)$ mode of phosphate groups [37] was also recorded, due to the presence of one molecular precursor (at trace levels), as the urease phosphate enzymatic substrate. The analysis of the lattice phonons region reveals, however, some peculiar features (Figure 7). The lattice vibration bands are wider and shift to lower frequencies

compared to those of the original fragment (Table 1). These features can be attributed to the diminution of the particles size which affects the force constant and vibrational amplitudes of the nearest neighbor bond and weakening of the crystal field [33, 34].

Table 1. Peak positions/cm⁻¹ and FWHM (cm⁻¹, in parenthesis) for Raman internal ν_1 and lattice active modes of pure calcite nanoparticles; plaster fragment and plaster treated with CaCO₃ nanoparticles.

Sample	ν_1	Lattice mode
CaCO ₃ (A) nanoparticles	1084.9 (10.0)	279.0 (24.5)
Original fragment	1085.8 (6.7)	281.5 (13.3)
Filled fragment	1084.7 (9.6)	277.9 (24.0)

Finally, the colour measurements are carried out to evaluate the effects of the 'filler' treatment based on CaCO₃ in the plaster samples. The colour is measured with a portable and miniaturized spectrophotometer according to the procedure previously described. It must be recalled that a total colour difference (ΔE) < 1, is not distinguished by the human eye; values in the range 1 < ΔE < 3, are regarded as clinically acceptable, whereas ΔE > 3.3 refers the appearance is not acceptable clinically [35].

Table 2. Colour alteration based on the total colour difference (ΔE), according to the Cielab [35].

Samples	ΔE	Acceptable values
Original no damaged plaster from ISCR	0.76±0.42	Reference sample
No-treated plaster from Palazzetto Lancia	1.47±0.72	Clinically acceptable
Treated plaster with CaCO ₃ nano-Filler	1.54±0.60	Clinically acceptable
PLA/MMT7 coating agent [35]	4.93±0.96	Not clinically acceptable
Aged 1000h_1% Cu + 2% a.a. + 2% salt	5.59±0.82	Not clinically acceptable
1000h Tego + 3% Yb	5.40±0.93	Not clinically acceptable
1000h Tego + 3% Yb+30% TEOS	5.70±0.85	Not clinically acceptable

The colorimetric measurements reported in Table 2, together with reference values, confirm that the CaCO₃ (A) sample induces the best recovery of the initial chromatic properties. These conclusion come from the values obtained for the ΔE^* parameter which are smaller than those obtained with a reference plaster sample and other substrata treated with different fillers and/or consolidating agents, widely described in literature [35].

4. Conclusions

In this study the CaCO₃(A) nanoparticles were applied, as filler, for the damaged plaster samples, that came from the Palazzo Lancia, a Renaissance palace, located in San Salvatore in Campo (Rome). TEM results showed that the CaCO₃ (A) nanoparticles (synthesized by the enzymatic approach) resulted very

well controlled in their shape and size. The TEM micrographs also revealed that the aggregation effects (due to the solvent evaporation during the sample preparation for the TEM observation) are limited and very similar to the evaporation phenomena that occurred during the plaster fragments restoration with the CaCO₃ nano-filler. The application of the nanoparticles in alcoholic medium on the plaster fragment surfaces was analytically monitored by SEM (under a morphological point of view), EDAX (for the elemental compositional analysis), by the Hg porosimetry and the WAC test. The WAC test highlighted that a natural transpiration of water was also guaranteed avoiding the hydro repellent behaviour (typical for the polymers, traditionally applied as consolidating agents). All data demonstrated the efficiency of the CaCO₃ as nano-filler for the damaged plaster fragments, and especially the μ -Raman spectroscopy clearly showed the presence of the nanoparticles into the plaster substrata. Further quantitative evidences, for the presence of nanoparticles into the plaster surfaces, comes from the EDAX measurements where a significant increase of the Ca/Mg ratio was found. The characterization of the mechanical properties of the plaster fragment, after the CaCO₃ based treatments, was carried out by the STT assay. The total recovery of the robustness and stability of the plaster surfaces had been also achieved by applying the CaCO₃ nano-filler.

Acknowledgment

The authors wish to thank Mrs. Cadia D'Ottavi for the XRD technical support and assistance and for fruitful comments and suggestions. Thanks are also due to the Dr. C.S. Salerno (from the ISCR, Rome) and Dr. Antonella Docci (from the ISCR, Rome & Masterpieces, s.r.l.; <http://www.masterpiecesrl.it/>) for providing sample fragments, essential to carry out all the entire study.

References

- [1] P. Baglioni, R. Giorgi and L. Dei, *Chimie*, **12** (2009) 61-69.
- [2] R. Giorgi, M. Baglioni, D. Berti, and P. Baglioni, *Accounts Chem. Res.*, **43** (2010) 695-704.
- [3] E. Carretti, M. Bonini, L. Dei, B.H. Berrie, L.V. Angelova, P. Baglioni and R.G. Weiss, *Accounts Chem. Res.*, **43** (2010) 751-760.
- [4] P. Baglioni, D. Chelazzi, R. Giorgi, and G. Poggi, *Langmuir*, **29** (2013) 5110–5122.
- [5] P. Baglioni and R. Giorgi, *Soft Matter.*, **2** (2006) 293–303.
- [6] P. Baglioni and D. Chelazzi, *Nanoscience for the Conservation of Works of Art*, RSCA Nanoscience & Nanotechnology, No. 28, The Royal Society of Chemistry, London, 2013.
- [7] M. Favaro, R. Mendichi, F. Ossola, S. Simon, P. Tomasin and P.A. Vigato, *Polym. Degrad. Stabil.*, **92** (2007) 335–351.
- [8] M. Favaro, R. Mendichi, F. Ossola, U. Russo, S. Simon, P. Tomasin and P.A. Vigato, *Polym. Degrad. Stabil.*, **91** (2006) 3083–3096.
- [9] V. Horie, *Materials for Conservation: Organic consolidants, adhesives and coatings*, 2nd edn., Butterworth-Heinemann - Elsevier, London, 2010.

- [10] M. Ambrosi, L. Dei, R. Giorgi, C. Neto and P. Baglioni, *Langmuir*, **17** (2001) 4251–4255.
- [11] M. Ambrosi, L. Dei, R. Giorgi, C. Neto and P. Baglioni, *Prog. Coll. Pol. Sci. S.*, **118** (2001) 68-72.
- [12] A. Nanni and L. Dei, *Langmuir*, **19** (2003) 933–938.
- [13] R. Giorgi, L. Dei and P. Baglioni, *Stud. Conserv.*, **45** (2000) 154–161.
- [14] R. Giorgi, L. Dei, M. Ceccato, C. Schettino and P. Baglioni, *Langmuir*, **18** (2002) 8198–8203.
- [15] P.N. Manoudis, I. Karapanagiotis, A. Tsakalof, I. Zuburtikudis, B. Kolinkeová and C. Panayiotou, *Appl. Phys. A*, **97** (2009) 351–360.
- [16] P. Marconi, *Le facciate dipinte cinquecentesche a Roma: problemi di storiografia artistica e di conservazione*, Atti del convegno di studi, G. Rotondi & M.G. Branchetti (eds.), Rizzoli, Genova, 1982, 127-131.
- [17] I. Belli Barsali, *Facciate dipinte nelle ville romane*, Atti del convegno di studi, G. Rotondi & M.G. Branchetti (eds.), Rizzoli, Genova, 1982, 39-41.
- [18] M.J. Mosquera, D.M. de los Santos, A. Montes and L. Valdez-Castro, *Langmuir*, **24** (2008) 2772–2778.
- [19] I. Sondi, D.S. Skapin and B. Salopek-Sondi, *Crys. Growth Des.*, **8** (2008) 435-441.
- [20] R.K. Pai and S. Pillai, *Cryst. Eng. Comm.*, **10** (2008) 865-872.
- [21] Y. Ocak, A. Sofuoglu, F. Tihminlioglu and H. Böke, *Prog. Org. Coat.*, **66** (2009) 213–220.
- [22] D. De Angelis, U. Barberini and C.B. Ridolfini, *Le case romane con facciate graffite e dipinte*, Editore Amici dei Musei di Roma, Roma, 1960, 89-123.
- [23] R. Kultzen, *Relazione e proposte al problema della graduale rovina degli affreschi rinascimentali sulle facciate delle case romane*, Atti del convegno di studi, G. Rotondi & M.G. Branchetti (eds.), Rizzoli, Genova, 1982, 37-38.
- [24] C. Conti, C. Colombo, D. Dellasega, M. Matteini, M. Realini and G. Zerbi, *J. Cult. Herit.*, **12** (2011) 372–379.
- [25] M. Sadat-Shojai and A. Ershad-Langroudi, *J. Appl. Polym. Sci.*, **112** (2009) 2535–2551.
- [26] R. Jenkinsa, T.G. Fawcetta, D.K. Smitha, J.W. Vissera, M.C. Morrisa and L.K. Frevela, *Powder Diffr.*, **1** (1986) 51-63.
- [27] J. Bochen, S. Gil and J. Szwabowski, *Cement Concrete Comp.*, **27** (2005) 769–775.
- [28] T. Kanti Sen and K.C. Khilar, *Adv. Colloid Interfac.*, **119** (2006) 71–96.
- [29] E. Carretti, D. Chelazzi, G. Rocchigiani, P. Baglioni, G. Poggi and L. Dei, *Langmuir*, **29** (2013) 9881–9890.
- [30] P. Mora and G. Torracca, *Bollettino Istituto Centrale Del Restauro*, (1965) 109-132.
- [31] V. Daniele and G. Taglieri, *J. Cult. Herit.*, **11** (2010) 102-106.
- [32] V. Daniele and G. Taglieri, *J. Cult. Herit.*, **13** (2012) 40-46.
- [33] D.C. Smith and C. Carabatos-Nédelec, *Raman spectroscopy applied to crystals: phenomena and principles, concepts and conventions*, in *Handbook of Raman Spectroscopy. Practical Spectroscopy*, I.R. Lewis & H.G.M. Edwards (eds.), Marcel Dekker, New York, 2001, 349-422.
- [34] G. Gouadec and P. Colomban, *Prog. Cryst. Growth Ch.*, **53** (2007) 1-56.
- [35] L. Yue, M. Shui and Z. Xu, *Spectr. Lett.*, **34** (2001) 793-802.
- [36] M. De La Pierre, C. Carteret, L. Maschio, E. André, R. Orlando and R. Dovesi, *J. Chem. Phys.*, **140** (2014) 164509-164520.
- [37] J. Xu, I.S. Butler and D.F.R. Gilson, *Spectrochim. Acta Part A*, **55** (1999) 2801–2809.